Proceedings of the ASME 2012 Conference on Smart Materials, Adaptive Structures and Intelligent Systems
SMASIS2012
September 19-21, 2012, Stone Mountain, Georgia, USA

SMASIS2012-7917

SIMULATION OF INTERACTION BETWEEN LAMB WAVES AND CRACKS FOR STRUCTRUAL HEALTH MONITORING WITH PIEZOELECTRIC WAFER ACTIVE SENSORS

Yanfeng Shen Victor Giurgiutiu
Laboratory for active materials and smart structures, University of South Carolina, Columbia, South Carolina, USA

ABSTRACT

In this paper, the detection for two kinds of cracks is studied: (1) linear notch crack; (2) nonlinear breathing crack. A pitch-catch method with piezoelectric wafer actives sensors (PWAS) is used to interrogate an aluminum plate with a linear notch crack and a nonlinear breathing crack respectively as two cases. The inspection Lamb waves generated by the transmitter PWAS, propagate into the structure, interact with the crack, acquire crack information and are picked up by the receiver PWAS. The linear notch crack case is investigated through: (1) analytical model developed for Lamb waves interacting with a general linear damage; (2) finite element simulation. The breathing crack, which acts as a nonlinear source, is simulated using two approaches: (1) element activation/deactivation technique; (2) contact model. The theory and solving scheme of the proposed element activation/deactivation approach is discussed in detail. The signal features of different damage severities are analyzed. Crack opening, closing, stress concentration, surface collision phenomena are noticed for the breathing cracks. Mode conversion is noticed for both crack cases. The generation mechanism and mode components of the new wave packets are investigated by studying the particle motion through the plate thickness. A damage index is proposed based on the spectral amplitude ratio between the second harmonic and the excitation frequency for the breathing crack. The damage index is found capable of estimating the presence and severity of the breathing crack. The paper finishes with summary and conclusions.

INTRODUCTION

Cracks, even at their early stage, exist as considerable menace to structural integrity. If not handled appropriately, they may end up with growing in an uncontrollable manner and cause structure malfunctions. Thus, a structural health monitoring strategy for detecting the presence and propagation of cracks is of importance to avoid catastrophic failures.

Piezoelectric wafer active sensors (PWAS) compared with conventional ultrasonic transducers are small, light-weight, unobtrusive transducers that can be permanently bonded on host structures and could be used both as sensors and actuators [1]. In plate structures, PWAS can generate Lamb waves, which have been studied as a powerful tool to inspect plate structures due to their nice features of long propagating distance. When Lamb waves arrive at structural defects, such as cracks, fatigue or plastic zone, they will interact with these structural changes, and be modified by the defects and carry the information along with them. A pitch catch method is usually used to obtain the structural change information between a transmitter and a receiver [2]. In this study, a pitch catch method is used to study the interaction between Lamb waves and cracks.

When Lamb waves arrive at a crack, several phenomena may happen: transmitting of waves through the crack, reflection of waves by the crack, mode conversion, and even introduction of nonlinearity [3, 4]. After interaction with cracks, the received Lamb waves signal will have changes in amplitude, generation of new wave packets or introduction of nonlinearity. The analytical solution of PWAS generated Lamb waves propagating in pristine plates have been developed in previous work [5, 6]; but the analytical model of a general linear damage with transmission, reflection, mode conversion capability is not included. In this paper, an analytical model of Lamb waves interacting with a linear damage is built; the results are compared with solutions from finite element simulation.

Breathing cracks are nonlinear sources in wave propagation. At a breathing crack, nonlinearity will be introduced into the inspection waves. Experiments have demonstrated the capability of nonlinear Lamb waves to detect structural defects. But most of the studies on nonlinear ultrasonics to date have been experimental and on non-dispersive waves like longitudinal bulk waves or Rayleigh waves [7-9]. Few predictive studies exist, especially for Lamb waves. In this paper, the nonlinear Lamb waves generated from interaction

between Lamb waves and the breathing crack is simulated with finite element method via two methods: (1) element activation/deactivation approach; (2) contact model. A damage index is proposed based on the spectral amplitude ratio between the second harmonic and the excitation frequency for the breathing crack. The damage index is found capable of estimating the presence and severity of the breathing crack.

ANALYTICAL MODEL OF LAMB WAVES INERACTING WITH LINEAR DAMAGE

A pitch-catch method is used to investigate the interaction between Lamb waves and cracks. A typical pitch-catch configuration between a transmitter PWAS and a receiver PWAS is shown in Figure 1.

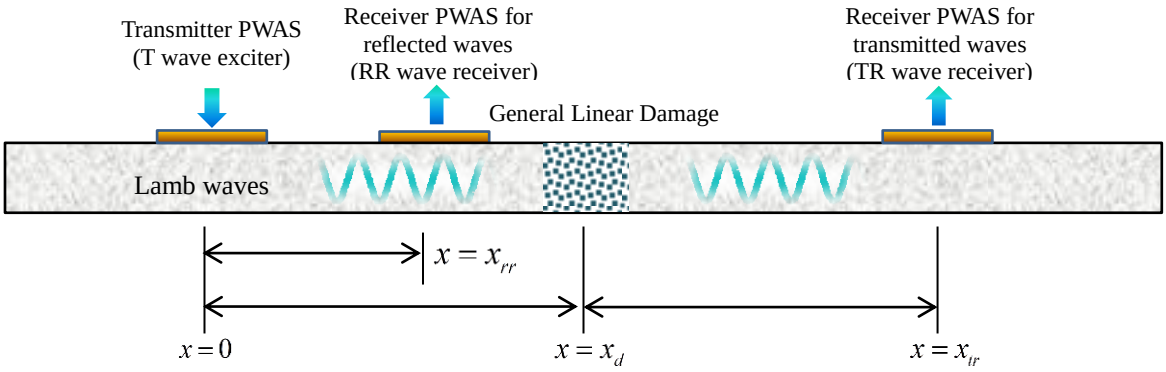

Figure 1: A pitch-catch configuration between a transmitter PWAS and a receiver PWAS

The analytical modeling of pitch-catch Lamb waves interacting with a linear damage is carried out in frequency domain. The modeling process could be described in four main steps:

(1) Fourier transform the time-domain excitation signal $V_e(t)$ into frequency domain signal $\tilde{V}_e(\omega)$;

(2) Multiply the frequency domain excitation signal with plate transfer function until the damage location $G(\omega, x_d)$, and obtain the signal just at the damage location as $V_d(\omega, x_d) = G(\omega, x_d) \cdot \tilde{V}_e(\omega)$; The plate transfer function is given by

$$G(x,\omega) = S(\omega) e^{-i\xi^S x} + A(\omega) e^{-i\xi^A x} \tag{1}$$

where

$$S(\omega) = \kappa_{PWAS} \sin \xi^S a \frac{N_S(\xi^S)}{D_S'(\xi^S)} \tag{2}$$

$$A(\omega) = \kappa_{PWAS} \sin \xi^A a \frac{N_A(\xi^A)}{D_A'(\xi^A)} \tag{3}$$

Where ξ is the frequency dependent wave number of each Lamb wave mode and the superscripts S and A refer to symmetric and antisymmetric Lamb wave modes. The notations of ref. **Error! Reference source not found.**, page 321-329 are adopted. κ_{PWAS} is the complex transduction coefficient that converts applied strain into PWAS voltage. The modal participation functions $S(\omega)$ and $A(\omega)$ determine the amplitude of the S0 and A0 wave modes excited into the structure. The terms $\sin(\xi^S a)$ and $\sin(\xi^A a)$ control the tuning between the PWAS transducer and the Lamb waves with PWAS size a. Hence, the signal at the damage is

$$V_d(x,\omega) = S(\omega)\tilde{V}_e(\omega) e^{-i\xi^S x_d} + A(\omega)\tilde{V}_e(\omega) e^{-i\xi^A x_d} \tag{4}$$

(3) The signal at the damage location will now act as a new wave source, and transmission, reflection and mode conversion will happen here. When S0 mode waves arrives at the damage, part of them will be transmitted through the crack as S0 mode waves, some will be reflected as S0 waves, part will undergo mode conversion and be transmitted as A0 mode, and some may be reflected as A0 mode; when A0 mode waves arrives at the damage, part of them will be transmitted as A0 mode waves, some of them will be reflected as A0 modes, part of them will undergo mode conversion and be transmitted as S0 mode waves and some will be reflected as S0 mode waves. Thus we define the transmission, reflection coefficient of S0 and A0 waves and mode converted wave transmission and reflection coefficients as SST, SSR, AAT, AAR, SAT, SAR, AST, ASR. In step three the amplitudes are assigned to each wave component. From this new source, Lamb waves will propagate and be linearly added together to obtain the final frequency domain wave signal at the receiver PWAS. The whole ideal is based on principle of superposition of linear systems. The final forms of frequency domain signals at the receiver for transmitted and reflected waves are

$$
\begin{aligned}
V_{tr}(\omega, x_r) = {} & SST \cdot S(\omega)\tilde{V}_e(\omega)e^{-i\xi^S x_d} \cdot e^{-i\xi^S (x_{tr}-x_d)} \\
& + SAT \cdot S(\omega)\tilde{V}_e(\omega)e^{-i\xi^S x_d} \cdot e^{-i\xi^A (x_{tr}-x_d)} \\
& + AAT \cdot A(\omega)\tilde{V}_e(\omega)e^{-i\xi^A x_d} \cdot e^{-i\xi^A (x_{tr}-x_d)} \\
& + AST \cdot \tilde{V}_e(\omega)e^{-i\xi^A x_d} \cdot e^{-i\xi^S (x_{tr}-x_d)}
\end{aligned} \tag{5}
$$

$$
\begin{aligned}
V_{rr}(\omega, x_r) = {} & S(\omega)\tilde{V}_e(\omega)e^{-i\xi^S x_{rr}} + A(\omega)\tilde{V}_e(\omega)e^{-i\xi^A x_{rr}} \\
& + SSR \cdot S(\omega)\tilde{V}_e(\omega)e^{-i\xi^S x_d} \cdot e^{-i\xi^S (x_d - x_{rr})} \\
& + SAR \cdot S(\omega)\tilde{V}_e(\omega)e^{-i\xi^S x_d} \cdot e^{-i\xi^A (x_d - x_{rr})} \\
& + AAR \cdot A(\omega)\tilde{V}_e(\omega)e^{-i\xi^A x_d} \cdot e^{-i\xi^A (x_d - x_{rr})} \\
& + ASR \cdot \tilde{V}_e(\omega)e^{-i\xi^A x_d} \cdot e^{-i\xi^S (x_d - x_{rr})}
\end{aligned} \tag{6}
$$

In equation (5) and (6), we can see the wave components are linearly added; in equation (6), the first line is the direct incident wave from the transmitter, other four lines are the reflected terms including reflected waves from mode conversion.

(4) The frequency domain signal at the receiver is inverse Fourier transformed back into time domain and can be written as $V_R(t, x_r) = IFFT\{V_r(\omega, x_r)\}$

FINITE ELEMENT MODEL OF LAMB WAVES INTERACTING WITH LINEAR NOTCH CRACK AND NONLINEAR BREATHING CRACK

Finite Element Model of Linear Notch Crack

The finite element model for this study is shown in figure 2. The linear notch crack is simulated by deactivating the selected thin layer of elements at the crack location.

In our model, two $7\text{mm} \times 7\text{mm} \times 0.2\text{mm}$ piezoelectric wafer active sensors (PWAS) are considered ideally bonded on a 2-mm thick aluminum plate. One PWAS works as a transmitter and sends tone burst excitation signal into the structure; the other PWAS transducer functions as receiver and detects the wave signal arriving in at the receiver locations. The plate is long enough to ensure the received signals are not influenced by boundary reflections. The distance between the transmitter PWAS and the receiver PWAS transducer is shown in Figure 2. The crack is located at 200 mm from the transmitter, such that the S0 and A0 wave packets have already separated when Lamb wave arrives at the crack location; hence the S0 and A0 wave packets interact with the breathing crack individually, which allows us to see how the crack influences differently the S0 and A0. The crack size is 1.2 mm through the thickness.

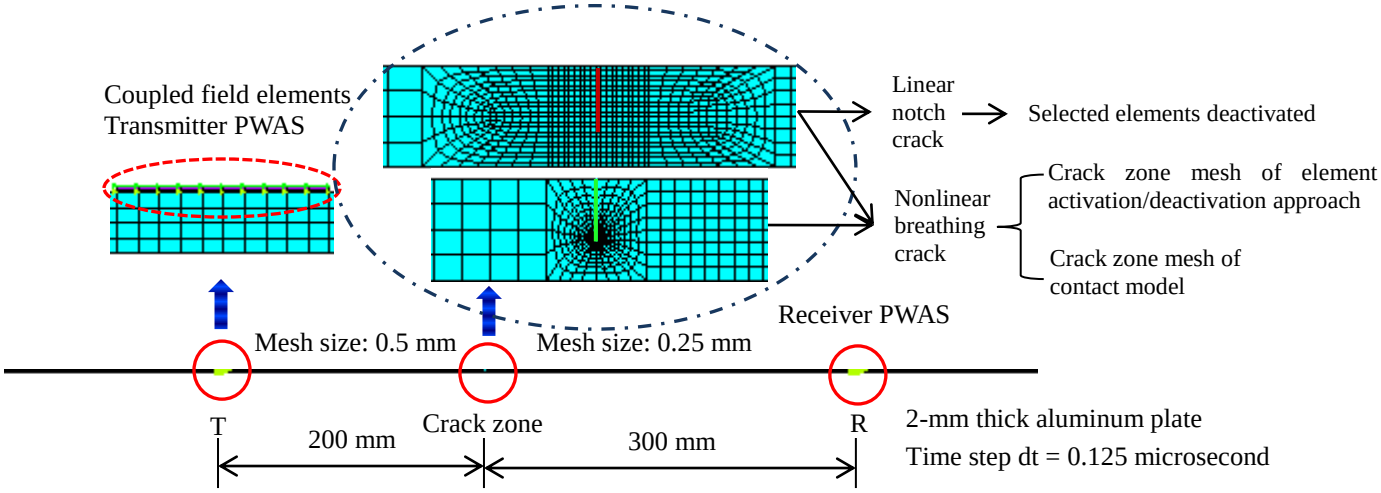

Figure 2. Finite element model used for linear notch crack and nonlinear breathing crack

The model is a 2D transient problem under the plane strain assumption to simulate a pitch-catch SHM process. The PWAS transducers are modeled with coupled field elements (PLANE13) which couple the electrical and mechanical variables (ANSYS 13.0 Multi-Physics). The plate is modeled with four nodes structure element PLANE182 with "element birth and death" capability. A 20 volts peak to peak 5-counts Hanning-window modulated tone burst signal centered at 100 kHz is applied on the top electrode of the transmitter PWAS. The plate is under free boundary condition. The Lamb waves sent out by transmitter PWAS will propagate along the plate, interact with the crack, pick up crack information, and be detected by the receiver PWAS

Finite Element Model of Nonlinear Breathing Crack

We use two methods to model the nonlinear breathing crack: (1) element activation/deactivation approach; (2) contact model. The main layout (plate material and geometry, PWAS and crack locations, excitation, etc.) of the finite element model is the same as that of the linear notch crack model shown in figure 2. The main difference is when we simulate the nonlinear breathing crack, the selected thin layer of elements do not stay

deactivated, but undergo activation and deactivation cycles. And for the contact model, contact elements are used to model the contact surfaces of the breathing crack. In the contact model, elements CONTA172 and TARGE169 are used to construct the contact pairs.

Since we are interested in the relationship of damage severity and the nonlinearity of the wave signal, we modify the damage severity of the plate, which is represented by the number of elements selected to be deactivated and reactivated in the element activation/deactivation approach. We define the damage severity as the index where $r = a/h$ (a and h are the crack size and plate thickness respectively). An index of $r = 0.0$ corresponds to pristine condition, where there is no crack in the plate. In our simulation, we used 20 elements across the thickness at the crack zone. Different damage severities $r = 0.0, 0.5, 0.4, 0.3, 0.2, 0.1$ and 0.0 were generated by selecting 12, 10, 8, 6, 4, 2 and 0 elements to be deactivated and reactivated. For the contact model, the damage severity is controlled by changing the crack geometry.

LINEAR NOTCH CRACK RESULTS

For the linear notch crack case, the finite element simulation of a pristine plate is carried out to compare with the cracked plate signal. The time domain simulation signal at the receiver is shown in figure 3 for $r = 0.6$ situation and pristine case.

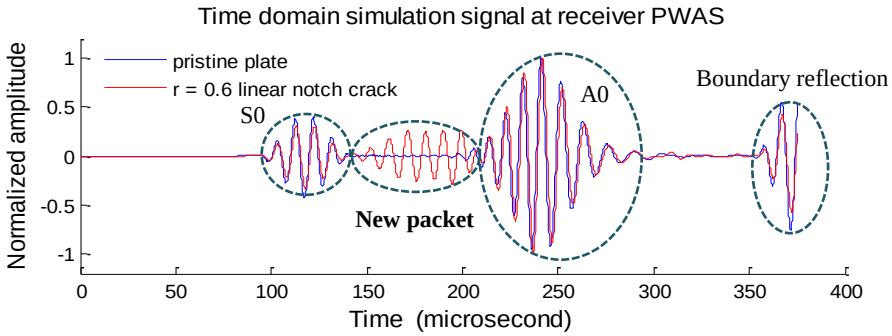

Figure 3. FEM simulation signal at receiver PWAS

Figure 3 shows two wave packets, S0 and A0, and the boundary reflection. Compared with pristine case, the linear notch crack signal has a new packet. This new packet is generated at the crack due to mode conversion. However, we do not know the mode component in the new packet. One benefit of finite element method is that it allows us to obtain the solutions at any location within the analyzed body. So, at the sensing location, the nodal strain at the up most point and down most point across the thickness is obtained to get information about the mode component of the coming waves. As shown in figure 4, S0 and A0 mode components could be separated.

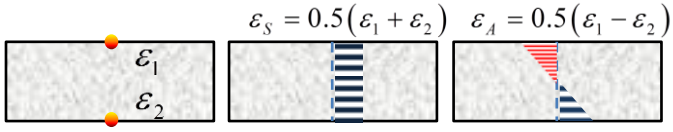

Figure 4 Separation of S0 and A0 Lamb modes

Upon separation, the time domain simulation signal is decomposed into pure S0 mode waves, pure A0 mode waves, and total waves; they are shown in figure 5.

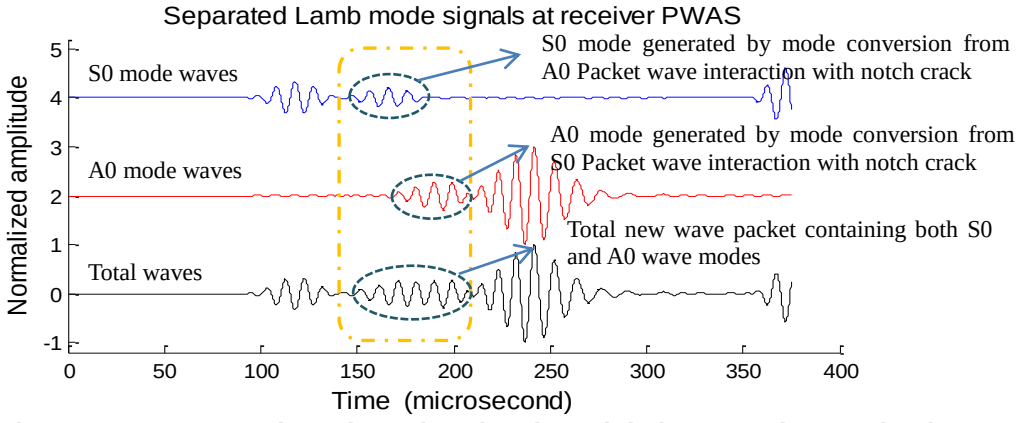

Figure 5. Decomposed Lamb modes signals and their generation mechanism

The results from finite element simulation are compared with the analytical model developed. For the linear notch crack, the finite element simulation result of $r = 0.6$ and the analytical

solution based on the idea of generalized linear damage are shown in figure 6. We can see that the results from finite element simulation and the analytical model agree with each other very well. S0 and A0 packets have very high degree of agreement; the new packet has a slight phase difference, but the main trend matches very well.

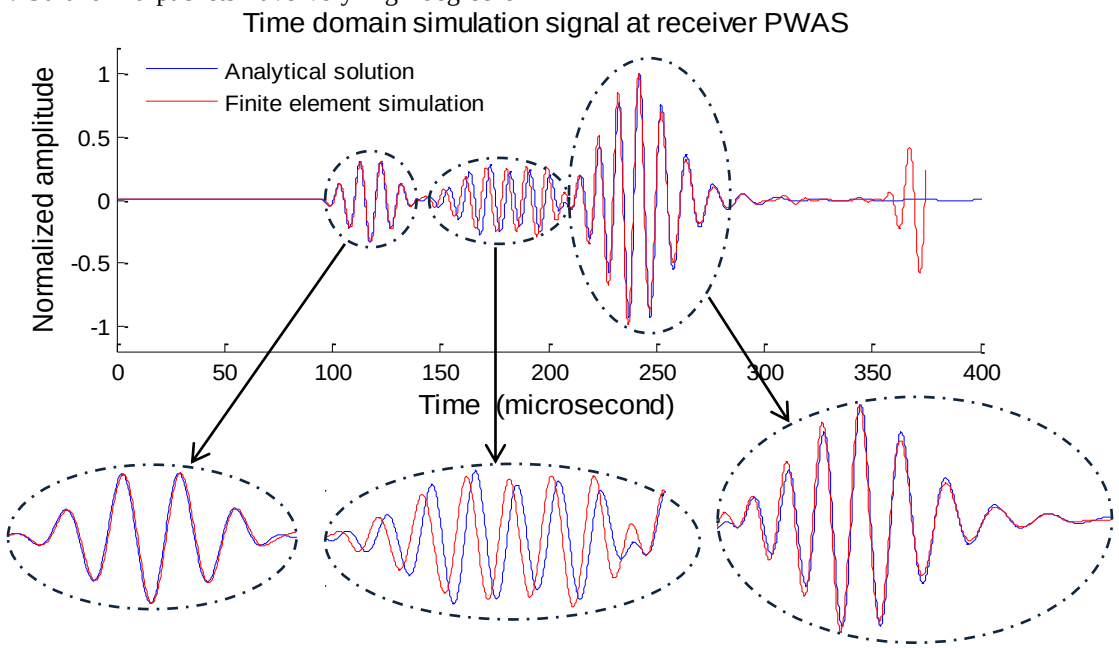

Figure 6 Comparison of finite element simulation results with analytical model

NONLINEAR BREATHING CRACK RESULTS

Results of Nonlinear Breathing crack

As mentioned in the previous section, simulations of different damage severity cases were carried out with $r = 0.6, 0.5, 0.4, 0.3, 0.2, 0.1$ and 0.0. For $r = 0.6$, the nonlinear effect should be the most obvious, therefore this case was used as a representative for nonlinear effect. It was observed that the crack opening, closing, stress concentration and crack surface collision could be noticed. The situations of crack open and close for both S0 and A0 modes are shown in Figure 7 The same crack behavior could be observed from both the element activation/deactivation approach and contact model that under tension, the crack opens, and stress concentration could be observed at the crack tip; it is apparent that the tension part of the Lamb wave does not penetrate the crack. When the compression part of the Lamb wave arrives, the crack closes, and collision between "crack surfaces" is noticed; hence, the compression part of the Lamb wave can penetrate into the crack..

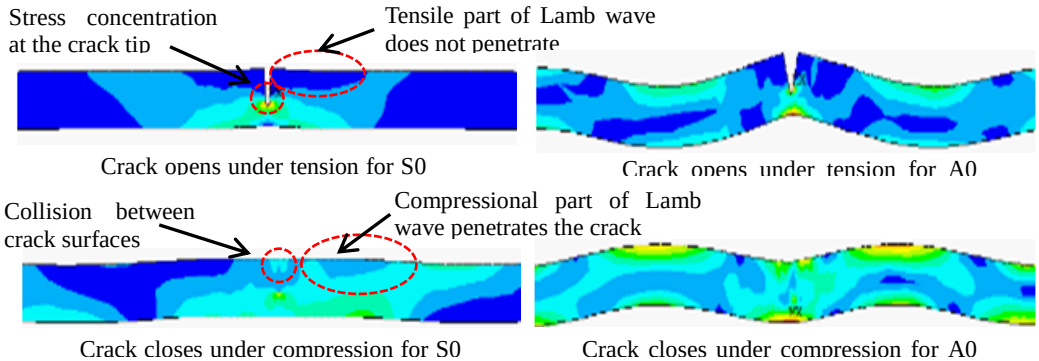

Figure 7. Breathing crack opens and closes for S0 and A0 modes (r = 0.6)

The superposed time domain simulation signals of pristine case, nonlinear breathing crack case at receiver PWAS are shown in Figure 8. It can be observed that compared with pristine condition, the nonlinear cracked plate signal has a slight amplitude drop and phase shift in both S0 and A0 packets. Another difference is that a new wave packet appears due to the existence of crack. This new packet is a special feature introduced by mode conversion at the breathing crack: when

the crack is opened, no matter by the S0 or A0 packet, the effect of tension force at the crack location could be decomposed into stretching force and bending moment w.r.t the neutral axis, which will generate correspondingly S0 and A0 mode components. When the crack closes, since the crack surfaces have relative velocity, collision between the crack surfaces will happen. The effect of this collision could also be decomposed into two parts: compression force and bending moment, which will generate respectively S0 and A0 components. From the analysis of mode component in the precious section, it can be concluded that the new packet contains both S0 and A0 mode waves. Fourier transforms of S0, A0 and the new wave packets are carried out, and plotted in Figure 9.

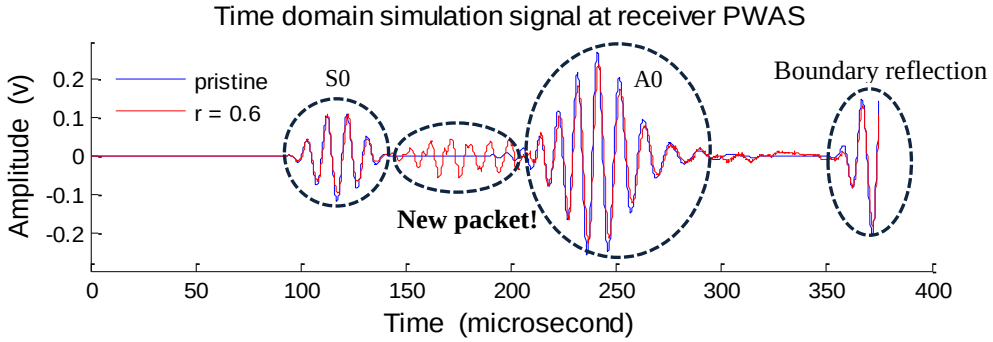

Figure 8. Superposed time domain simulation signals of pristine plate and nonlinear breathing crack case

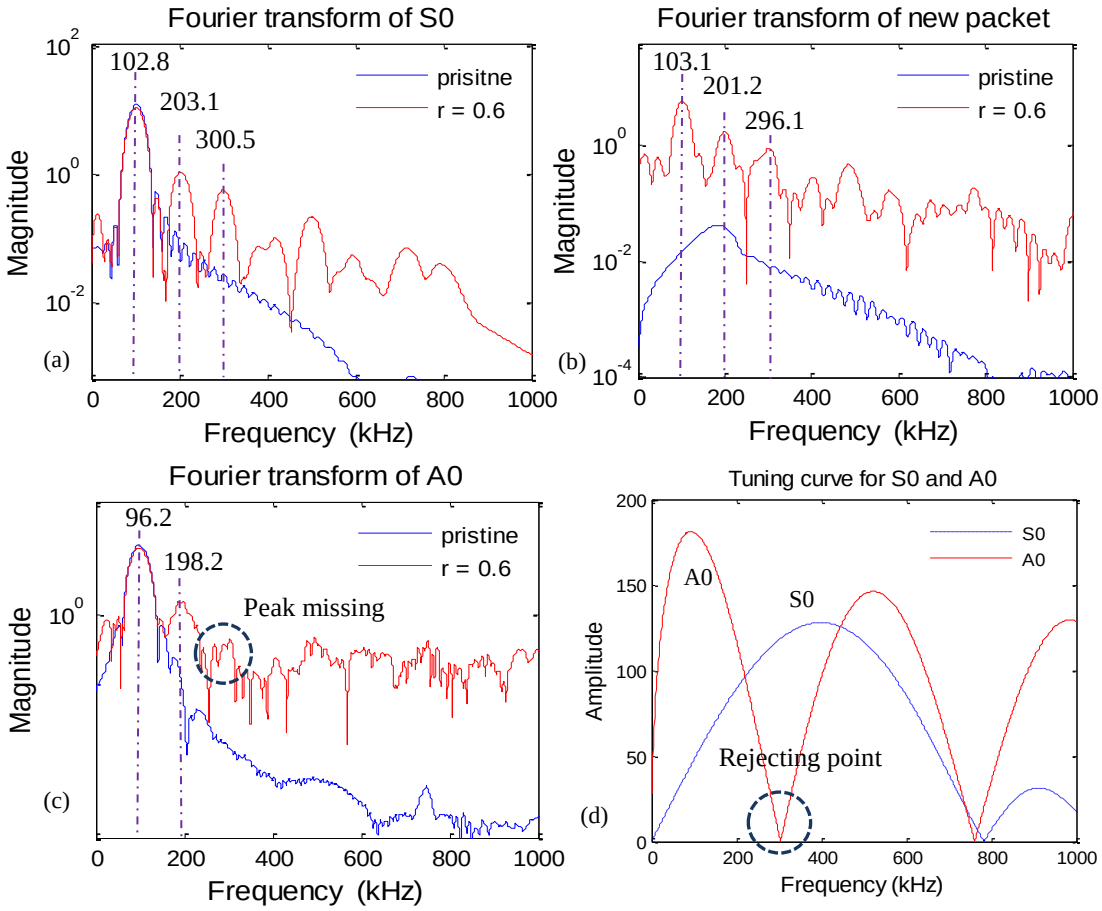

Figure 9. Fourier transform of S0, A0 and the new packet: (a) S0; (b) new packet; (c) A0; (d) tuning curves for A0 and S0

For all the wave packets, the pristine signal does not shown any higher frequency components whereas the signal from nonlinear breathing crack plate shows distinctive nonlinear higher harmonics. Figure 8a shows distinctive nonlinear higher harmonics in the S0 wave packet. Since the excitation frequency is centered at $f_c = 100$ kHz, the 102.8 kHz peak corresponds to the excitation frequency f_c, and the 203.1 kHz, 300.5 kHz correspond to $2f_c, 3f_c$ respectively. For the A0 wave packet (Figure 8c), the first peak corresponds to the excitation frequency f_c, and the second harmonic $2f_c$ could be clearly observed at 198.2 kHz, but the third harmonic $3f_c$ is somehow missing. This phenomenon is due to the tuning effect of PWAS and plate structure combination [10]. The tuning curve shown in Figure 9d indicates that at around 300 kHz, where the third harmonic should appear, the A0 mode reaches its rejection point; In other words, for the given PWAS and plate structure, this frequency could not be detected due to the rejection effect at the receiver PWAS. Analysis of the observed "new packet" (Figure 9b) also reveals the nonlinear higher harmonics pattern for the nonlinear breathing crack case. The peaks of the breathing crack frequency domain signal correspond to excitation frequency f_c, nonlinear higher harmonics $2f_c, 3f_c, 4f_c$ and $5f_c$. In this new packet, the feature of nonlinear higher harmonics seems to be more obvious than in the S0 and A0 packets. And the amplitudes of the higher harmonics are closer to that of the excitation.

To further identify the damage severity, the simulation results from $r = 0.6, 0.5, 0.4, 0.3, 0.2, 0.1$ and 0.0 are compared for the breathing crack case. The amplitude ratio of second harmonic to excitation frequency is adopted to show the degree of nonlinearity, which may serve as a damage index indicating damage severity, i.e.

$$DI = \frac{A(2f_c)}{A(f_c)} \tag{7}$$

where $A(f_c)$ and $A(2f_c)$ denote the spectral amplitude at the excitation frequency and at the second harmonic in the frequency domain. The variation of DI with crack damage severity is shown for S0 and A0 packets in Figure 10a and for the new packet in Figure 10b. It can be observed in Figure 10 that the amplitude ratio DI is relatively small for both S0 and A0 packets, but it is quite big for the new wave packet even at small values of r. The DI for S0 and A0 has a monotonically increasing relationship with the crack damage intensity. So the ratio DI from the new packet could serve as an early indicator for the presence of a breathing crack, and the ratio DI for the S0 and A0 packets can serve as an indicator of damage severity.

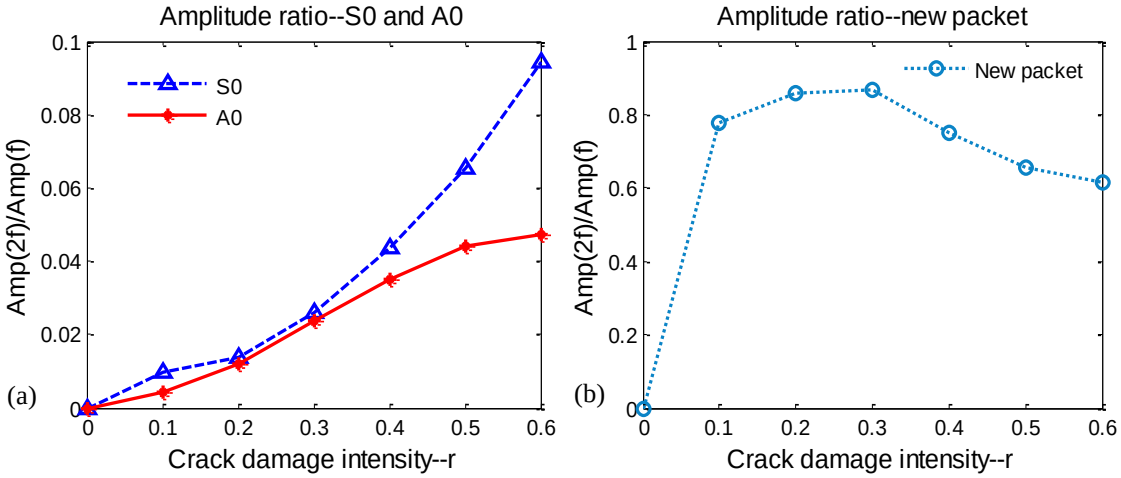

Figure 10. Damage severity index

Comparison between Element Activation/deactivation Approach and Contact Model

To evaluate the element activation/deactivation approach, the calculation results are compared with those obtained from contact model. The superposed time domain simulation signals and frequency spectrum from the two methods for $r = 0.6$ case are shown in figure 11a and 11b to compare the results and evaluate the closeness of the two methods.

Figure 11 shows that the solutions from these two methods agree very well with each other, the main characteristics of all the wave packets are the same. S0 packet has better accuracy; A0 and new packet have slight phase and amplitude difference. In the frequency spectrum, it could be noticed that at low frequency the two methods agree with each other very well, but at high frequency they deviate more from each other. Since the interested frequency range is first and second harmonic, at this range, two solutions match with each other well.

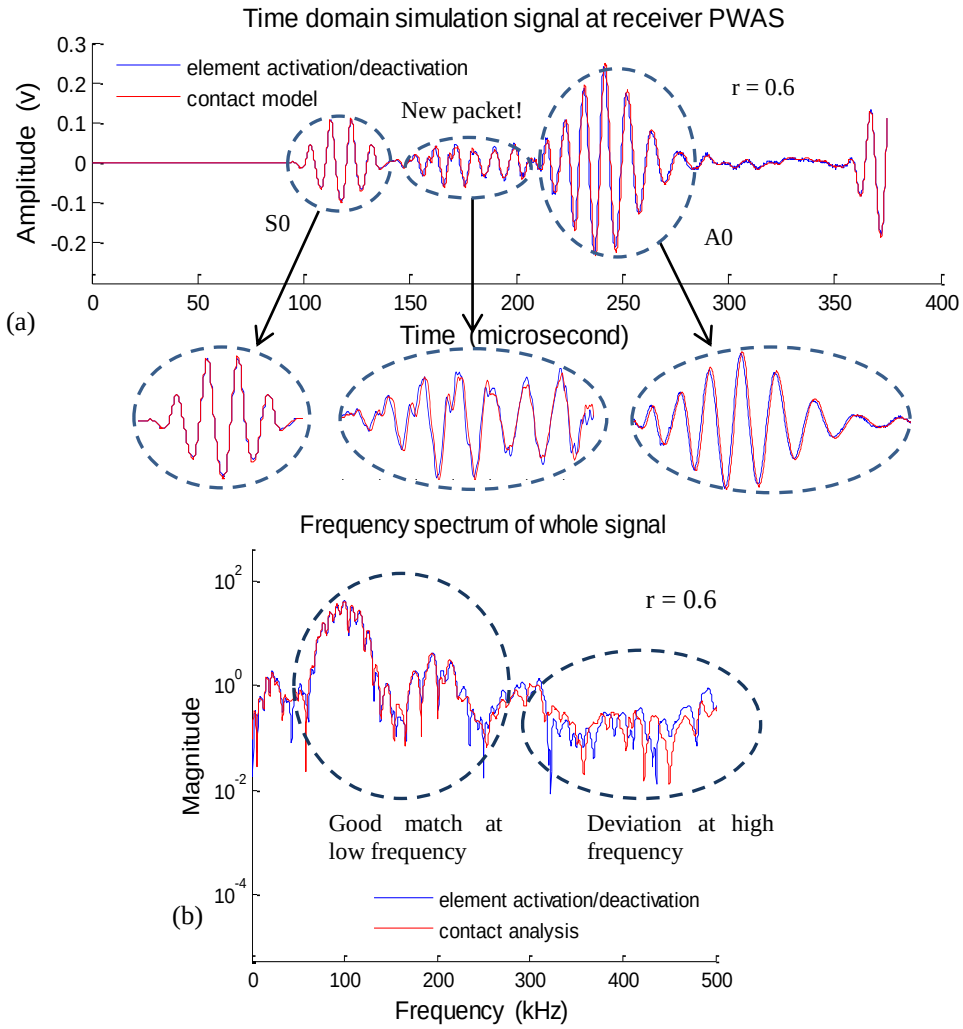

Figure 11. Comparison between signals from element activation/deactivation approach and contact model (a) time domain signal; (b) frequency spectrum.

The error or "difference" between two solutions are measured and presented by the L_2 norm [11]

$$\|u_e - u_c\| = \sqrt{\sum_1^N (u_e - u_c)^2} \tag{8}$$

Where u_e and u_c are the solutions from element activation/deactivation approach and contact analysis; N is the number of solution points in the time domain signal. The errors for $r = 0.1, 0.2, 0.3, 0.4, 0.5, 0.6$ cases are plotted in figure 12. It could be observed that the element activation/deactivation approach is stable for all the crack geometries; for all the damage severity cases, both methods match well with each other.

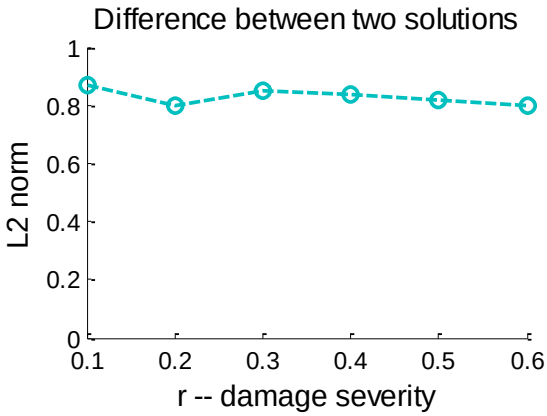

Figure 12 Difference between two solutions for various damage severities

SUMMERY AND CONCLUSSIONS

In this paper, we presented predictive simulation of interaction between Lamb waves and cracks. The Lamb wave interaction with linear notch crack is simulated with analytical model and the finite element method. The analytical model is developed in frequency domain with the idea of general linear damage with wave transmission, reflection and mode conversion properties. New wave packet is observed due to mode conversion at the crack. And results from the analytical model and the finite element simulation agree with each other very well.

The Lamb wave interaction with nonlinear breathing crack is simulated with finite element method via two ways: (1) element activation/deactivation approach; (2) contact model. The results show the element activation/deactivation method agrees well with the contact analysis and is capable of simulating the nonlinear behavior of breathing cracks. Besides S0 and A0 packets, a new packet is observed in the time domain signal due to the presence of the breathing crack. The nonlinear phenomenon of higher harmonics can be noticed in the frequency spectrum of all the wave packets. This distinctive feature allows us to tell the presence of cracks initiated in structure components. Different cases with various damage severities are investigated and compared. A damage index is proposed based on harmonics spectrum amplitude ratio. This damage index is found to increase monotonically with damage for the S0 and A0 wave packets. However, for the new wave packet, this damage index is very sensitive to low damage values, but does not increase thereafter. Using this damage index, we find that the new packet is more sensitive to the presence of the crack, while S0 and A0 packets can provide monitoring information on the severity of damage growth.

Comparing the linear notch crack signal with the nonlinear breathing crack signal, it is noticed that the linear notch crack signal takes smooth and regular waveform in all the wave packets; however, the nonlinear breathing crack signal is distorted in waveform for both S0 and A0 packets and the new packet is heavily distorted with zigzags in waveform. It is also found that compared with the notch crack, the S0 waveform of the breathing crack have bigger amplitude, meaning the breathing crack has a bigger S0 wave transmission coefficient. For the new packet, linear crack wave has bigger amplitude than the nonlinear breathing crack, meaning at the notch crack more mode conversion will occur.

ACKNOWLEDGMENTS

Support from Office of Naval Research #N00014-11-1-0271, Dr. Ignacio Perez, Technical Representative; Air Force Office of Scientific Research #FA9550-11-1-0133, Dr. David Stargel, Program Manager; are thankfully acknowledged.

REFERENCES

[1] Giurgiutiu, V., 2007, “Structural Health Monitoring with Piezoelectric Wafer Active Sensors,” Academic Press,

[2] Giurgiutiu, V. 2010, “Structural Health Monitoring with Piezoelectric Wafer Active Sensors – Predictive Modeling and Simulation”, INCAS Bulletin, Vol. 2, No. 3, 2010, pp. 31-44

[3] Cho, Y., 2004, "Estimation of Ultrasonic Guided Wave Mode Conversion in a Plate with Thickness Variation," IEEE Transactions on Ultrasonics, Ferroelectrics, and Frequency Control, vol. 47, no. 3,

[4] Shen, Y., Giurgiutiu, V., 2012, “Predictive Simulation of Nonlinear Ultrasonics,” Proc. SPIE, Paper No. 8348

[5]Giurgiutiu, V., Gresil, M., Lin, B.; Cuc, A., Shen, Y., Roman, C., 2012, “Predictive Modeling of Piezoelectric Wafer Active Sensors Interaction with High-frequency Structural Waves and Vibration,” Acta Mechanica, online first 10.1007/s00707-012-0633-0

[6] Gresil, M., Shen, Y., Giurgiutiu, V., 2011, “Predictive Modeling of Ultrasonics SHM with PWAS Transducers,” Proceedings of the 8th International Workshop on Structural Health Monitoring, 2011, 13-15 September 2011, Stanford University, CA

[7] Viswanath, A., Rao, B., Purna, C., Mahadevan, S, 2010, “Nondestructive Assessment of Tensile Properties of Cold Worked AISI Type 304 Stainless Steel Using Nonlinear Ultrasonic Technique,” Journal of materials processing technology, Vol. 211, Issue 3, 538-544

[8] Nagy, B. P., 1998, “Fatigue Damage Assessment by Nonlinear Ultrasonic Materials Characterization,” Ultrasonics, Vol. 36, 375-381

[9] Hermann, J., Jacobs, L. J., Qu, J., Kim, J. Y., 2006, “Generation and Detection of Higher Harmonics in Rayleigh Waves Using Laser Ultrasound, Review of Quantitative Nondestructive Evaluation,” Vol. 25,pp. 262-269

[10] Giurgiutiu, V., 2005, “Tuned Lamb wave excitation and detection with piezoelectric wafer active sensors for structural health monitoring, Journal of intelligent material systems and structures, “, Vol. 16, No.4, pp. 291-306

[11] Reddy, J. N., *An introduction to the finite element method*, Tata McGraw-Hill edition